# Book of Tutorials and Abstracts

European
Microbeam Analysis Society

University of
BRISTOL

Mineralogical Society

# EMAS 2018

## 13th EMAS Regional Workshop

## MICROBEAM ANALYSIS IN THE EARTH SCIENCES

4 - 7 September 2018
University of Bristol, Wills Hall, Bristol, Great Britain

Organised in collaboration with:
Mineralogical Society of Great Britain and Ireland
and
University of Bristol

# ELECTRON PROBE MICROANALYSIS (EPMA) IN THE EARTH SCIENCES

R.D. Walshaw

University of Leeds, School of Earth & Environment, Leeds Electron Microscopy & Spectroscopy Centre
Woodhouse Lane, Leeds LS2 9JT, Great Britain
e-mail: r.d.walshaw@leeds.ac.uk

## 1. INTRODUCTION

Electron probe microanalysis (EPMA) is a non-destructive, standards-based microanalytical technique, yielding fully quantitative chemical analyses of solid materials at the micron scale. It delivers accuracy and precision in the 1 - 2 % range and detection limits down to the ppm level. As many geochemical phenomena of mineralogical interest manifest at these scales and concentrations, EPMA is well suited to many fields of geological analysis. Consider in addition the technique's relatively high throughput, and it is easy to see why EPMA has become a central tool within the petrologists' arsenal.

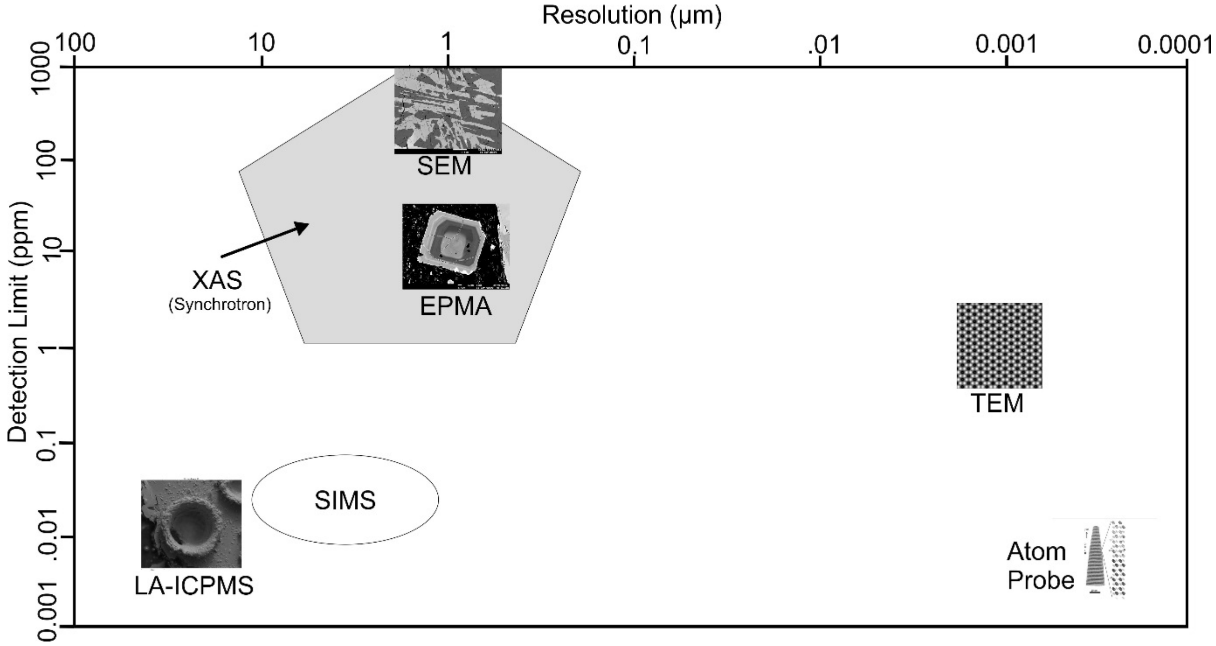

Figure 1. The microanalytical landscape: Showing the spatial analytical resolution and detection limit in ppm of EPMA relative to other commonly used microanalytical techniques (scanning electron microscopy - SEM, transmission electron microscopy - TEM, X-ray absorption spectroscopy - XAS, laser-ablation inductively-coupled mass spectrometry – LA-ICPMS). While not superior in either resolution or detection limit, EPMA is very well suited to the analysis of major, minor and trace elements in geological materials.

## 2. THE BASICS OF EPMA

The technique, developed during the PhD research of Raymond Castaing, published in 1951 [1], uses X-ray spectrometers and a focussed beam of electrons to analyse X-rays generated within a solid, polished sample. X-ray spectrometers mounted to a typical EPMA or "microprobe" are of two types: energy-dispersive (EDS); and wavelength-dispersive (WDS). The EDS is a solid state device which sorts incident X-rays by energy, counts and plots the entire energy spectrum effectively simultaneously. It is well suited to major elements and those with atomic numbers from Na upward. WDS uses diffracting crystals with different d-spacings to preferentially select X-rays of specific wavelengths while suppressing all others. Diffracted X-rays are passed to a gas-filled, proportional counter for counting. Wavelength-dispersive spectra are thus plotted sequentially, as the diffracting crystal moves to different positions, satisfying the Bragg equation for different wavelengths as it does so. WDS function requires that for all spectrometer crystal positions, the distance between the crystal and the counter is identical to that between the sample (X-ray source) and the crystal. This requires that the sample, diffracting crystal and proportional counter all sit on a theoretical circle known as the Rowland circle (Fig. 2). The Rowland circles of modern instruments typically have radii between 100 - 140 mm.

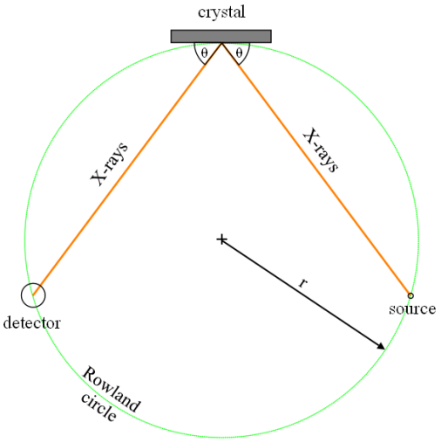

Figure 2. The Rowland circle of the wavelength-dispersive X-ray spectrometer.

It is the preferential selection of specific wavelengths over all others that gives WDS its superior peak to background ratio and thus lower detection limits when compared to EDS. It handles light elements and low concentrations much better than EDS, though, due to the problematic absorption of low energy X-rays within a sample, light element analysis should be considered non-trivial.

$$n\lambda=2d\sin\theta \qquad (1)$$

Equation 1. Braggs law of diffraction wherein: $n$ = the order of the reflection, $\lambda$ = the wavelength of the incident X-ray, $d$ = the inter-planar spacing (or d-spacing) of the diffracting crystal, $\theta$ = the glancing angle of the incident X-ray.

The ratio between background-corrected X-ray intensity for a given element $i$ in an unknown sample and that from a standard of known composition is known as the $k$-ratio ($k$). Castaing's first approximation states that the concentration of an element $i$ in a given unknown is approximately equal to $k$ multiplied by the concentration $C$ of the same element $i$ in the standard.

$$C_i^{unk} \approx \frac{I_i^{unk}}{I_i^{std}} C_i^{std} = K_i\, C_i^{std} \qquad (2)$$

Equation 2. Castaing's first approximation.

The reality is more complex than this due the effects of electron backscattering and inter-elemental absorption and fluorescence of X-rays within the matrix of a compound sample. These are known as "matrix effects" and the output from Castaing's first approximation is reduced, via a series of iterative calculations known as "matrix corrections" to arrive at a quantitative result within the commonly accepted 1 - 2 % accuracy range. Matrix corrections are complex and numerous, commonly used examples include ZAF, Phi Ro Z and XPP.

The instrumentation and methodology underpinning EPMA have been well developed in the 60 years since its inception, the underlying physics is well understood and it is safe to say EPMA is a mature analytical technique. That said, hardware, software and methods develop continually, opening up new analytical possibilities as they progress.

EPMA technique is now discussed in more detail using modern "state of the art" applications to illustrate its capabilities and limitations. The reader is referred to the standard texts of Reed [2] and Goldstein *et al.* [3] for additional detail.

## 3. *ANALYTICAL SPATIAL RESOLUTION*

Spatial resolution, or the smallest discrete volume of material which can be analysed, is governed by the atomic number (*z*) of the specimen material and the energy of the incident electron beam. It can be effectively modelled using Monte Carlo simulations (Fig. 3).

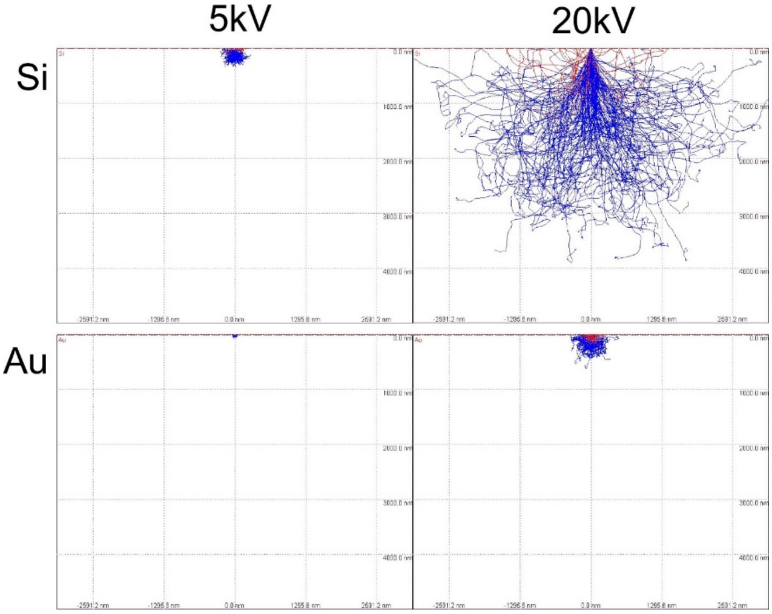

Figure 3. Monte Carlo simulations showing the electron-specimen interaction volumes produced by focussed electron beams at both 5 and 20 kV in pure silicon and pure gold. These volumes increase with increasing accelerating potential and decreasing atomic number.

EPMA is the characterisation of heterogeneity at the micron scale and characterisation of crystal zonation in igneous and metamorphic minerals is a common petrological application of the technique. Compositional differences between two regions of a crystal are commonly elucidated via a traverse of regularly spaced individual spot analyses (Fig. 4). Diffusion chronometry is a modern technique employed to elucidate the often short timescales of magmatic processes associated with volcanic eruption [4, 5]. EPMA is used to characterise diffusion-related zonation at the micrometre and nanometre scales. In certain instances the time resolution of the output magmatic timescales is directly related to the spatial resolution of the EPMA traverse. Spatial resolution when using a tungsten filament electron source under conventional conditions is constrained at between 2 - 5 µm for common silicates. Thus minimum spacing between adjacent analyses (e.g., in analytical traverses) is fixed within this range. Attempts to reduce such spacings result in the overlapping of individual interaction volumes.

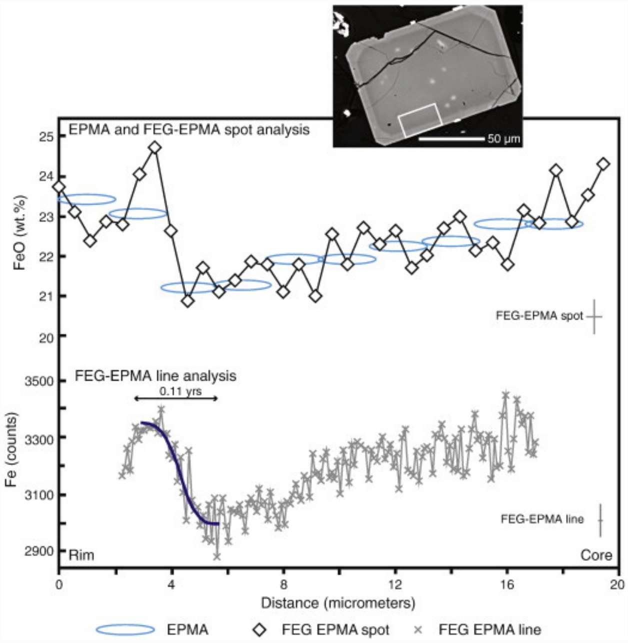

Figure 4. Comparison of the spatial resolution of high voltage EPMA and low voltage (LV) FEG EPMA in diffusion chronometry profiles in orthopyroxene (from [6]). The closer spacing within the LV FEG EPMA spot traverse yields considerably more information compared with the high voltage traverse.

The introduction of field emission gun (FEG) electron sources to EPMA instruments just over a decade ago, through their higher brightness and superior focus, has enabled the reduction of analytical volumes via the reduction of beam accelerating voltages, without any significant loss in X-ray signal from the sample. This in turn has enabled improved spatial resolution, allowing the analysis of sub-micron mineral inclusions and closer spacing in analytical traverses. The ability to make analytical traverses with spacings of less than 1um may result in order of magnitude improvement to the temporal resolution of the output, bringing it down, in the best case scenarios, from days to hours [6].

Reduction in accelerating voltage has a finite limit however. While selection of an accelerating voltage of 5 kV would in most silicates yield a total interaction volume of a few hundred nanometres, only lower energy X-rays whose critical excitation energies are exceeded will be generated. Fe – a common constituent in most geological samples – is a fly in the ointment in this regard. With a critical excitation energy ($E_c$) of 7.11 keV, the Kα X-ray will not be generated under such conditions. Adhering to a 5 kV accelerating potential would necessitate using the much less energetic Lα X-ray instead ($E_c = 0.70$ keV) which is highly problematic [7] and in the great majority of cases, unworkable. Instead of trying to achieve a small total excitation volume via unrealistic reduction in accelerating potential, workers in this area use what is termed the "low overvoltage" approach. Overvoltage is the difference between the energy of the incident beam electrons ($E_o$) and the excitation energy ($E_c$) of the characteristic x-ray of interest.

In conventional analysis with a tungsten filament source, overvoltage ratios ($E_o$ / $E_c$ ) of at least 2 are the norm, which in the case of Fe-Kα, necessitates using a 15 kV electron beam. Having different critical excitation energies, the individual X-rays of interest in any sample each have individual interaction volumes of differing dimension. This is due to attenuation of incident beam energy through sample interaction limiting the depth at which a given X-ray can be generated. Once the energy of a decelerating electron falls beneath the threshold $E_c$ for a given element, that element will cease to be excited within the sample. This means that x-ray generation is stratified, or contoured within the total interaction volume according to critical excitation energy and that a suitably small excitation volume can be achieved for the more energetic X-rays such as Fe and Mn by nature of their excitation being confined within the uppermost few nm of the specimen (Fig. 5).

Working at 8 kV is a compromise, but modern instrumentation is sufficiently stable to allow low overvoltage working and the acquisition of analyses – using Fe-Kα – from sub-micrometre volumes.

The adoption of the FEG into EPMA research has spawned the field of "low voltage EPMA" in which special consideration must be given to a number of factors considerably less important when working at higher accelerating voltages. These factors include carbon contamination, coating thickness (both of which attenuate signal from low energy X-rays), quantification using low-energy X-rays and the perennial challenge of standard selection [7-9].

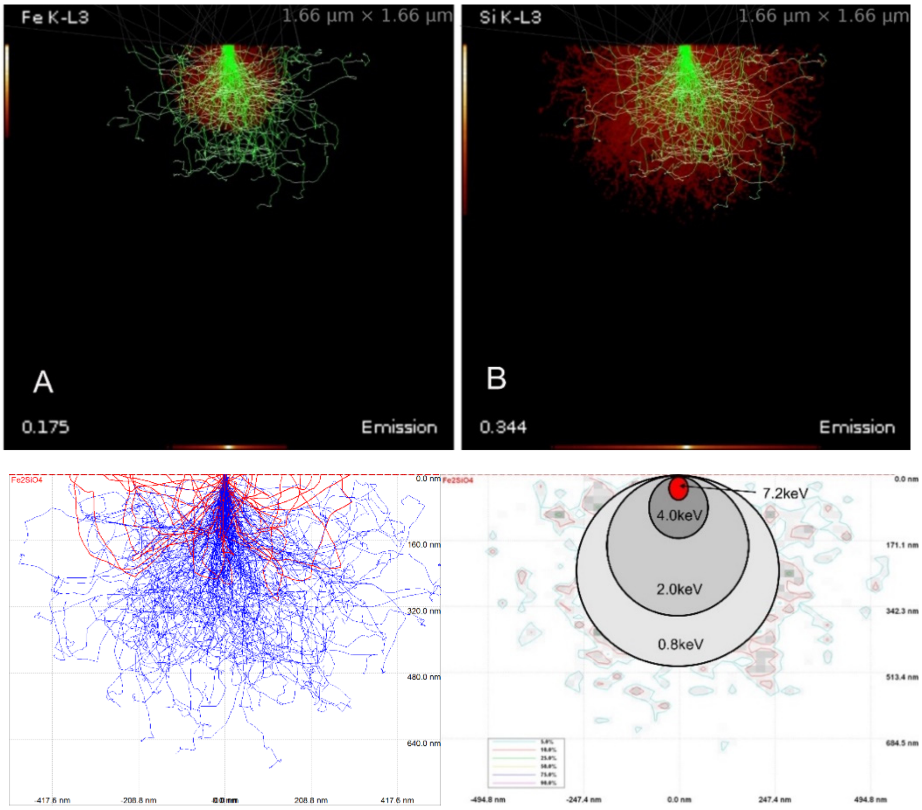

Figure 5. Monte Carlo simulations of electron interaction volume in Fayalite under an 8 kV beam. Excitation of Lα X-rays (green) takes place throughout the entire volume (red) (A), while most Kα excitation is confined within a small core region relative to the entire volume (B). (C) The same simulation shows the total interaction volume for fayalite at 8 kV to be approx. 650 nm in diameter. (D) Contouring of the penetrating, decelerating electrons by energy shows that energy very quickly falls below $E_c$ for Fe-kα and that these X-rays originate within a very small volume of approx. 80 nm (marked in red).

## *4. TRACE ELEMENT ANALYSIS*

### *4.1. Counting statistics*

When counting x-ray intensities, a total of 100,000 counts should be sufficient to achieve a 2σ uncertainty (two standard deviations = 95 % probability) of ± 0.6 % [2]. For typical major element count rates ($10^3$ - $10^4$ cps) this equates to count times of a few tens of seconds. Minor and trace elements will however produce significantly lower count rates (tens or hundreds of cps) under the same conditions and reaching the same 2σ precision at these count rates requires unattractively long count times. Strategies mitigating the need for such long counting times include increasing the count rate – typically by increasing the electron beam current (though this may create high detector dead times for the major elements) and counting a given element on multiple spectrometers and aggregating the counts.

### *4.2. Detection limit*

The smallest detectable peak is defined as having an intensity greater than or equal to three standard deviations (3σ) of that of the background. Detection limit (DL) is therefore heavily influenced by the uncertainty on the background determination. DL is inversely proportional to the square root of peak/background ratio (P/B), background corrected, on-peak count rate and counting time [3]. Increasing any of these by a factor of 4 will reduce DL by a factor of 2. Counting time and count rate (via beam current or accelerating voltage) are commonly increased as much as is reasonable when analysing trace elements. The Ti in quartz geothermometer [10] is a modern application of EPMA where detection limits of a few tens of ppm for Ti are required. Informed manipulation of the above analytical parameters on modern instruments with features such as large collection area diffracting crystals and h-type (high count-rate) spectrometers makes this achievable and the current best limit of detection for trace elements sits at around 10 ppm. Beyond this, users must consider alternate, mass-spectrometric techniques.

### *4.3. Background interferences*

Another challenging application of high precision, trace element analysis is the dating of monazite via the CHIME method [11, 12]. The technique requires the accurate, precise quantification of trace amounts of radiogenic Pb in the monazite matrix, along with its partner elements U and Th. The analysis is challenging due to the low concentrations involved and the manifold spectral interferences around the peaks of interest (Fig. 6). Other, mass-spectrometry techniques will yield better accuracy and precision with considerably less difficulty, however the small size of metamorphic monazites and the individual age domains contained within them mean that in certain instances, only EPMA can deliver the required spatial resolution. While detection limit and counting strategy remain vitally important, this application highlights the importance of choosing positions for background determination.

Traditional 2 point off-peak background determinations work very well in major element analysis where P/B are sufficiently high that the influence of small peak interferences on background positions are negligible (Figs. 5A and 5B). Where backgrounds show a high degree of curvature (Fig. 4C) and the presence of small interferences, often from higher order peaks, a greater degree of sophistication is required in selecting peak positions and interpolating background intensity beneath the peaks of interest. In the example of monazite dating, even a small error in background determination results in a significant error in the resultant age (Fig. 7) [13].

In such situations, the multipoint background approach of Allaz *et al.* [13] is very useful. Multiple positions can be selected for background determination, a statistical analysis of these points then allows the user to identify those points which represent real background and those which are artificially high due to subtle interference from higher order peaks. The compromised positions are rejected and the robust background positions are used to model background in the region of interest.

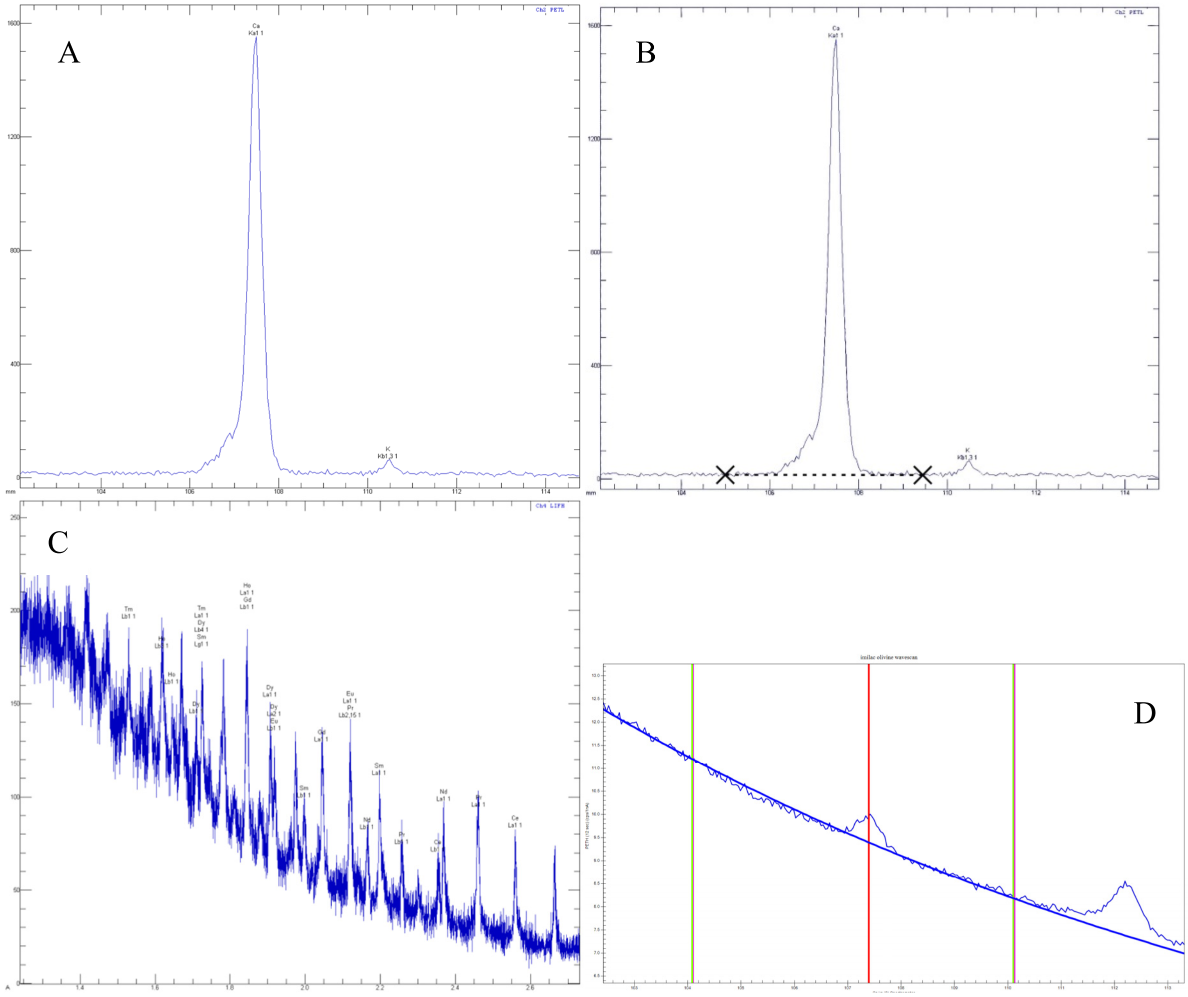

Figure 6. A) Wavelength dispersive spectrum showing the peak position for Ca Kα on a PET crystal. Peak to background ratio is in the order of 40 and the background is flat. B) Upper and lower background positions and the interpolated background position beneath the peak. C) Highly curved backgrounds require application of more sophisticated background models such as exponential or polynomial fits. The presence of numerous small peaks makes selection of clean background positions challenging. D) Exponential fit applied to a curved background under Ca-kα in olivine. Ca is present in trace quantities and such a background fitting approach is necessary to avoid serious overestimation of background intensity, which would result from a straight line fit.

## *5. HIGH SAMPLE THROUGHPUT*

An additional form of background determination, known as the Mean Atomic Number (MAN) background method [14], is an increasingly popular tool which significantly improves productivity via a 50 % reduction in analysis time.

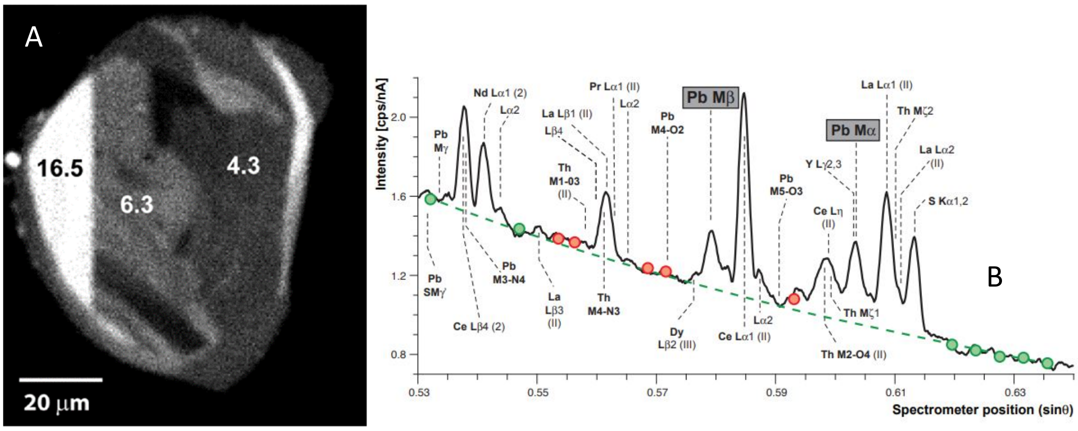

Figure 7. A) Zonation and Th concentrations in monazite (from [11]). Note small size, complexity and compositional variability of individual zones. B) Multipoint background applied to Pb-Mβ in monazite [13]. Red points = rejected, green points = accepted.

In MAN background analysis, the interdependence between background intensity and atomic number is exploited and backgrounds are not measured, but calculated instead. Integrating counts at the peak position for a given element, in a mineral standard *which contains a zero concentration of that element*, allows the user to directly determine background intensity at a given on-peak position for a given value of atomic number. Doing this for all elements of interest, in a range of standards with different mean atomic numbers bracketing the region of interest, allows the construction of a curve from which background intensity can be derived for any value of *z*-bar (Fig. 8). Use of this method cuts analysis time in half, as only on-peak intensities are measured. In the case of x-ray mapping, machine time can be reduced by 66 % as the requirement for running two off-peak background maps is removed and only the on-peak intensity map is collected.

## *6. BEAM SENSITIVE SPECIMENS*

Many common geological materials exhibit what is termed “beam sensitivity”, meaning that under electron beam irradiation they will in some way degrade or decompose. Several different mechanisms are covered by this portmanteau term including: dehydration; lattice damage (knock-on); Na migration; decarbonation; and on rare occasions, melting. Specimen decomposition during analysis is obviously undesirable and certain steps can be taken by the operator to mitigate or correct for the effects of this behaviour. Feldspars and volcanic glasses are common geological materials displaying beam sensitivity, Na – containing phases of this type are prone to Na loss. Beam interaction causes electron-implantation within the sample sub-surface and Na ions, due to their charge and small ionic radius will migrate out of the analytical volume, toward the negative charge [15]. Na rich compositions of feldspar and more acidic glasses display the strongest behaviour and the addition of an amount of water in rhyolitic glasses is a further complication (Fig. 9). Micas, phosphates, carbonates and sulphates are common mineral groups which also show beam sensitivity.

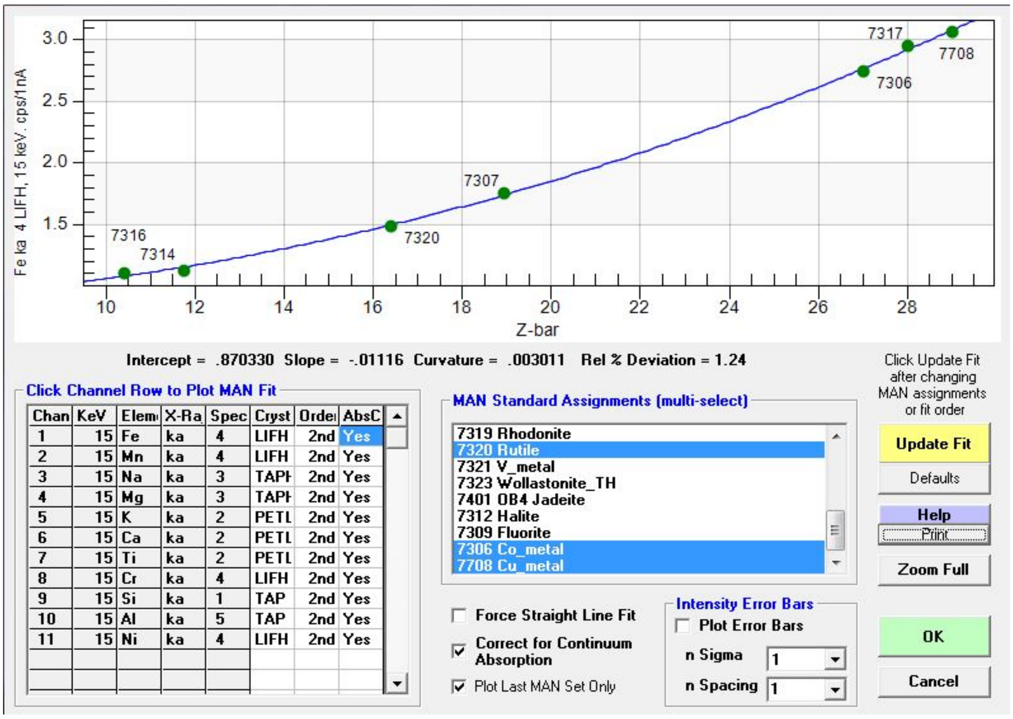

Intercept = .870330 Slope = -.01116 Curvature = .003011 Rel % Deviation = 1.24

Click Update Fit after changing MAN assignments or fit order

Click Channel Row to Plot MAN Fit

| Chan | KeV | Elem | X-Ra | Spec | Cryst | Orde | AbsC |
|---|---|---|---|---|---|---|---|
| 1 | 15 | Fe | ka | 4 | LIFH | 2nd | Yes |
| 2 | 15 | Mn | ka | 4 | LIFH | 2nd | Yes |
| 3 | 15 | Na | ka | 3 | TAPH | 2nd | Yes |
| 4 | 15 | Mg | ka | 3 | TAPH | 2nd | Yes |
| 5 | 15 | K | ka | 2 | PETL | 2nd | Yes |
| 6 | 15 | Ca | ka | 2 | PETL | 2nd | Yes |
| 7 | 15 | Ti | ka | 2 | PETL | 2nd | Yes |
| 8 | 15 | Cr | ka | 4 | LIFH | 2nd | Yes |
| 9 | 15 | Si | ka | 1 | TAP | 2nd | Yes |
| 10 | 15 | Al | ka | 5 | TAP | 2nd | Yes |
| 11 | 15 | Ni | ka | 4 | LIFH | 2nd | Yes |

MAN Standard Assignments (multi-select)

7319 Rhodonite
7320 Rutile
7321 V_metal
7323 Wollastonite_TH
7401 OB4 Jadeite
7312 Halite
7309 Fluorite
7306 Co_metal
7708 Cu_metal

☐ Force Straight Line Fit
☑ Correct for Continuum Absorption
☑ Plot Last MAN Set Only

Intensity Error Bars
☐ Plot Error Bars
n Sigma 1
n Spacing 1

Figure 8. A mean atomic number plot showing background intensity across a range of different values of mean atomic number (*z*-bar).

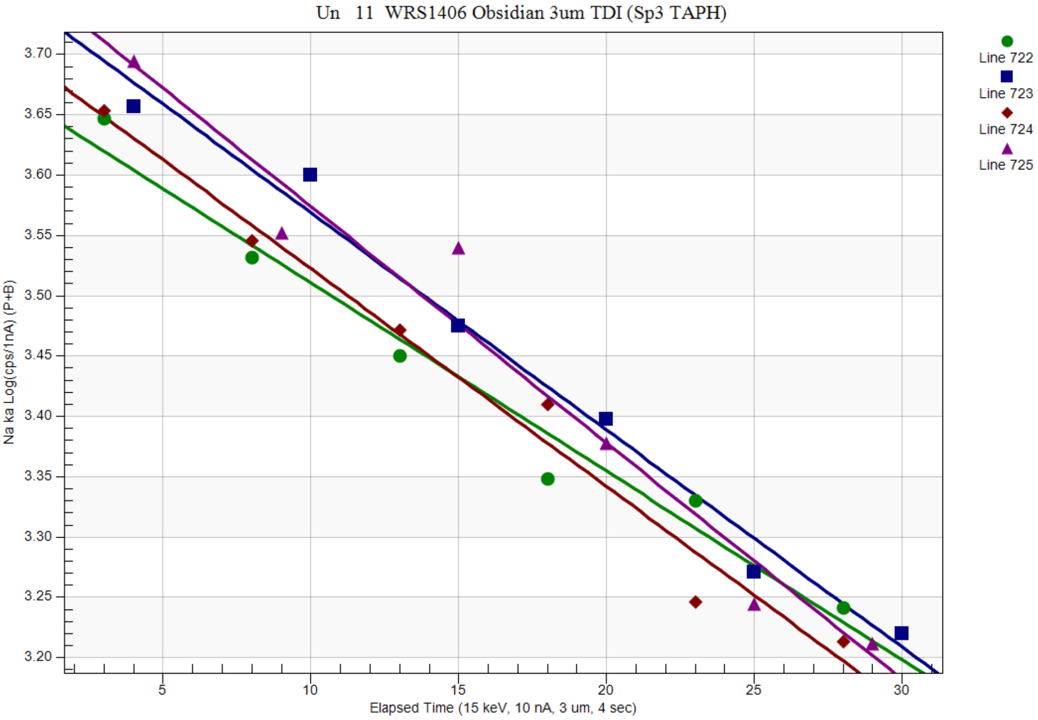
Un 11 WRS1406 Obsidian 3um TDI (Sp3 TAPH)

Figure 9. Time Dependant Intensity (TDI) plots for replicate analyses of Na in an obsidian. The data describe a drop in Na-Kα intensity of almost 20 % over 30 seconds.

The traditional strategy when analysing beam sensitive materials is to reduce the beam current and defocus the electron beam thus diffusing the beam energy, dropping the electron dose per unit area to a level at which beam damage is minimised or halted completely [15]. For many scenarios the appropriate beam conditions can be empirically established. It is also common to reduce on and off-peak count times, thus limiting the impact of any small amount of degradation. The combination of reduced beam currents and shorter count times will impact on counting statistics and the user may choose to accept poorer precision when working with this category of sample. It is also advisable in certain cases to choose very closely matched standards. If a mineral standard displays the same degradation behaviour as the unknown then the effects of beam sensitivity can, to an extent, be cancelled out.

An alternative approach, the Time Dependent Integration (TDI) method, first described by Nielsen and Sigurdsson [15] rather than preventing beam damage, aims to characterise and correct for it. Rather than integrating counts for a given element in one continuous packet, counts are integrated as a series of discrete pulses which capture any time-dependent decay in the count-rate of the target element. Plotting this decay then allows the user to back calculate to the correct intensity value for $T_0$.

The TDI approach allows the user to employ the higher beam currents and focussed electron beams that may be required to achieve a certain precision or spatial resolution, for instance during the analysis of very fine-grained crypto- tephra. TDI functions are now included within some EPMA software interfaces.

## *7. X-RAY MAPPING*

Additional to spot, or point analysis of discrete mineralogical features, X-ray compositional mapping of areas tens or hundreds of micrometres across is a common application of EPMA. The electron beam can be scanned across the area of interest, but to avoid artefacts associated with defocussing of WDS optics, it is more usual to scan the stage while keeping the beam fixed on-axis. X-ray intensities are plotted in x-y space as the stage moves, revealing the spatial distribution and relative abundances of the elements of interest. Major elements are often assigned to EDS while the WDS are reserved for the elements requiring greater sensitivity. Compositional maps may be qualitative (intensity only) or fully quantitative (Fig. 10). In both scenarios, the full suite of elemental X-ray intensities is acquired for each pixel, but in the latter, these intensities are then quantified against standardisations and matrix corrected in the normal way. Each pixel in the image is therefore a fully quantitative analysis, albeit with a very short count time and thus poor precision. The operator aims to lower DL and raise precision by increasing the pixel dwell time and beam current as high as is reasonably practicable. When mapping beam sensitive samples the usual constraints apply but a recent development in this area is the application of the TDI method to mapping (John Donovan, 2017 - Personal Communication). In both qualitative and quantitative mapping it is usual to collect an on-peak intensity map along with one or two off-peak background intensity maps, this is essential to allow background correction of on peak counts for quantitation, but also to remove mapping artefacts associated with jumps in background intensity between grains of different minerals, due to the strong interdependence (above) between background intensity and mean atomic number. As also discussed above, mean atomic number (MAN) background method is a tool which dramatically shortens the time needed for a mapping run as it removes the need to acquire background maps altogether.

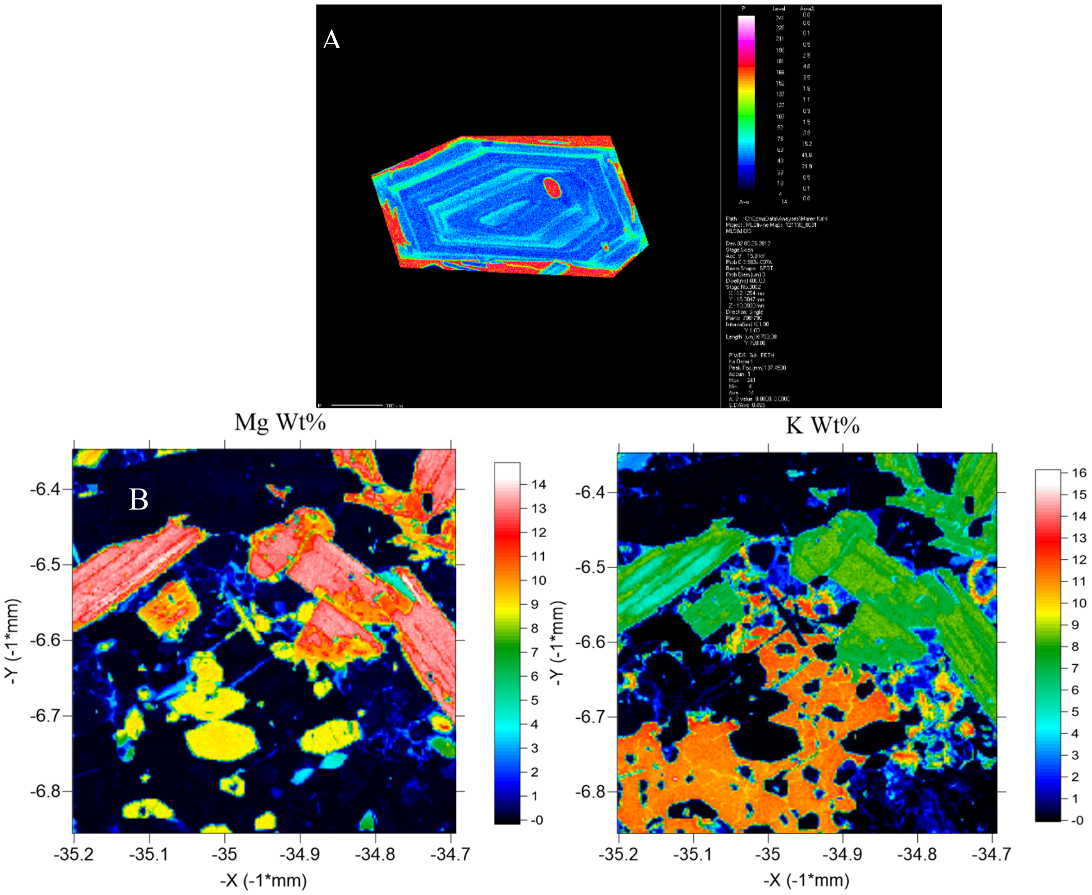

Figure 10. A) Qualitative intensity maps for P in olivine, P concentration approx. 200 ppm. B) Quantitative compositional X-ray maps for K and Mg in lamprophyre.

Users now commonly employ principal component analysis (PCA) to mine large, multispectral map datasets and extract cryptic information such as identification of minor mineral phases [16]. Modern instruments combining monochromated cathodoluminescence systems and soft-X-ray detectors with EDS and WDS offer hugely powerful hyperspectral data sets covering an extended proportion of the electromagnetic spectrum [17].

## *8. CONCLUSIONS*

EPMA is a well-founded, mature microanalytical technique, offering specific benefits over its higher precision partner techniques. Modern instrumentation and particularly software continue to develop opening up increasingly challenging and elucidating capabilities. In the hands of a well-trained operator, high quality analysis can be performed at sub-micron spatial resolutions with detection limits of tens of ppm. As research trends move to exploit these new capabilities, challenging EPMA work is becoming the new normal.

## *9. REFERENCES*

[ 1] Castaing R 1951 *PhD thesis*. (Paris, France: Université de Paris)

[ 2] Reed S J B 1975 *Electron microprobe analysis*. (Cambridge: Cambridge University Press)

[ 3] Goldstein J, Newbury D, Joy D, Lyman C, Echlin P E L, Sawyer L and Michael J 2003 *Scanning electron microscopy and X-ray microanalysis*. (New York, NY: Springer) 690

[ 4] Morgan D J, Blake S, Rogers N W, DeVivo B, Rolandi G, Macdonald R and Hawkesworth C J 2004 Time scales of crystal residence and magma chamber volume from modelling of diffusion profiles in phenocrysts: Vesuvius 1944. *Earth. Planet Sci. Lett.* **222** 933-946

[ 5] Pankhurst M J, Morgan D J, Thordarson T and Loughlin S C 2018 Magmatic crystal records in time, space, and process, causatively linked with volcanic unrest. *Earth. Planet Sci. Lett.* **493** 231-241

[ 6] Saunders K, Buse B, Kilburn M R, Kearns S and Blundy J 2014 Nanoscale characterisation of crystal zoning. *Chem. Geol.* **364** 20-32

[ 7] Buse B and Kearns S 2018 Quantification of olivine using Fe Lα in electron probe microanalysis (EPMA). *Microsc. Microanal.* **24** 1-7

[ 8] Buse B and Kearns S L 2014 Importance of carbon contamination in high-resolution (FEG) EPMA of silicate minerals. *Microsc. Microanal.* **20** 704-705

[ 9] Kearns S, Buse B and Wade J 2014 Mitigating thermal beam damage with metallic coats in low voltage FEG-EPMA of geological materials. *Microsc. Microanal.* **20** 740-741

[10] Wark D A and Watson E B 2006 TitaniQ: a titanium-in-quartz geothermometer. *Contrib. Mineral. Petrology* **152** 743-754

[11] Jercinovic M J and Williams M L 2005 Analytical perils (and progress) in electron microprobe trace element analysis applied to geochronology: Background acquisition, interferences, and beam irradiation effects. *Amer. Mineralogist* **90** 526-546

[12] Suzuki K and Kato T 2008 CHIME dating of monazite, xenotime, zircon and polycrase: Protocol, pitfalls and chemical criterion of possibly discordant age data. *Gondwana Res.* **14** 569-586

[13] Allaz J, Williams M L, Jercinovic M J and Donovan J J 2014 Trace element analyses by EMP: Pb-in-monazite and new multipoint background method. *Microsc. Microanal.* **20** 3

[14] Donovan J J and Tingle T N 1996 An improved mean atomic number background method for quantitative analysis. *J. Microscopy Soc. Am.* **2** 1-17

[15] Nielsen C H and Sigurdsson H 981 Quantitative methods for electron microprobe analysis of sodium in natural and synthetic glasses. *Amer. Mineralogist* **66** 547-552

[16] Buse B and Kearns S 2018 Evaluating X-ray microanalysis phase maps using principal component analysis. *Microsc. Microanal.* **24** 116-125

[17] MacRae C, Wilson N C, Torpy A and Pownceby M 2015 Cathodoluminescence and X-ray hyperspectral analysis in the FEG-EPMA. in: Book of Tutorials and Abstracts of the 14th European Workshop on Modern Developments and Applications in Microbeam Analysis. (Dresden, Germany: European Microbeam Analysis Society)